

Application of Fracture Mechanics to Strength Analysis of Glued Lap Joints*

K. KOMATSU** H. SASAKI** and T. MAKU**

Abstract—Strength of double lap joints of wood (Lawson cypress) including a glued end butt joint at center was analyzed by applying Fracture Mechanics. Approximate stress analysis was conducted in accordance with Volkersen type theory. Apparent strain energy release rate G^* of the joints was derived from applying the J-integral to the stress components. It was assumed that the apparent strain energy release rate G^* of the joints was proportional to the strain energy release rate G of cracked adhesive joint specimen subjecting to shear force and expressed as $G^*=NG$. Fracture criterion was assumed that when G^* reached its critical value $G^*_c (=NG_c)$, fracture occurred at the right-angled corner of the joints. Experimental results showed good applicability of derived equation on predicting strength of the joints when N was 0.5 and G_c was $0.25 \text{ kg}\cdot\text{cm}/\text{cm}^2$. A simple but conservative design equation between strength and the half lap length of the joints based on the experimental results and derived equation was proposed.

Introduction

In some recent studies on wood adhesion, fracture toughness G_c has been treated as characteristic value which dominates fracture of wood adhesive system^{1)~5)}. Fracture toughness is, as well known, a material parameter which dominates cohesive fracture of homogeneous materials with cracks, and has the unit of energy per area or force per length. Namely, this value can be interpreted either as specific energy spent by crack propagation of infinitesimal area or as specific force required to crack extension of infinitesimal length.

In research field of wood adhesion, this value is also understood as specific energy spent by separation of infinitesimal joint area, and it is expected that the higher this value is, the more tough the joint is. Studies presented in the past on this kind of subject were mainly focused on measuring fracture toughness of various wood adhesive system under various types of loading, but scarcely extended to the aspect of application. It is, however, presumed that this characteristic value will also play an important role in analyzing fracture of particular shaped part of bonded structure having steep stress concentration like right-angled corner.

In this study, double lap joints of wood including an end butt joint bonded with rigid epoxy adhesive were considered, and strength analysis of the joints was

* Presented partly at the 25th Annual Meeting of the Japan Wood Research Society, Fukuoka, April, 1975.

** Division of Composite Wood.

attempted by applying Fracture Mechanics. According to previous stress analysis⁶⁾, it is clear that there is a steep stress concentration at the tip of right-angled corner of the glued lap joints. This stress concentration accompanies also with a steep concentration of strain energy which equilibrates with specific energy calculated as the product of infinitesimal joint area and apparent strain energy release rate of the lap joints. Suddenly at the instance of breakdown of this energy balance, fracture occurs at the tip of the right-angled corner. In order to examine the qualitative presumption mentioned above, an attempt of estimating apparent strain energy release rate of double lap joints was made by applying the J-integral method derived by Rice^{7,8)} and it was assumed that fracture started when the apparent strain energy release rate reached its critical value peculiar to the right-angled corner. As this critical value of the apparent strain energy release rate has not been obtained yet, it was assumed that the value was proportional to the fracture toughness obtained on the specimen having sharp cracks along glue lines and subjected to shear force.

Theory

Derivation of Critical Axial Stress of Double Lap Joints.

Fig. 1 is schematic explanation of glued double lap joint specimen subjected

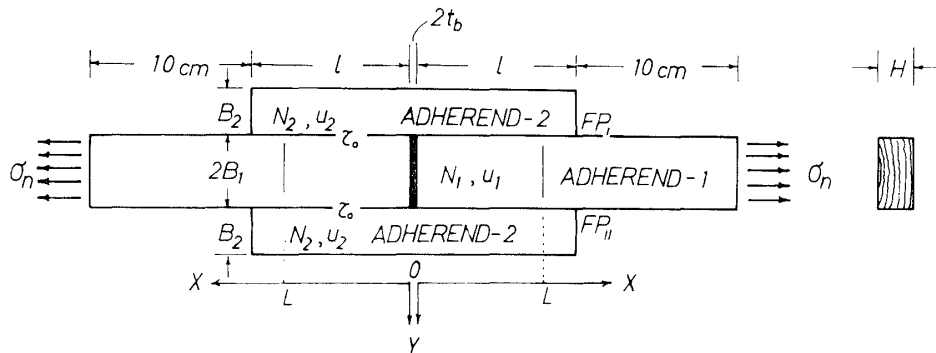


Fig. 1. Double lap joints specimen including a butt joint at the center. $2t_b$ is thickness of gap or glue line of the butt joint. Lines at $x=L$ indicate the location of knifeedge of the extensometer. Two corner points FP_I and FP_{II} are thought to be most critical for fracture initiation.

to uniform tensile stress σ_n at both ends of the center adherend. Apparent axial forces N_1 and N_2 in adherends, apparent displacements u_1 and u_2 of adherends, and apparent shear stress τ_0 in glue line obtained by approximate method of analysis similar to Volkersen type procedure⁶⁾, are as follows (see APPENDIX about the details):

$$N_1 = \sigma_n \alpha H \left\{ \frac{\psi_1 \sinh k(x-l) + \psi_2 \sinh kx + \psi_3 \cosh kx}{\psi_2 \sinh kl + \psi_3 \cosh kl} + \beta \right\}, \quad (1)$$

$$N_2 = \sigma_n \alpha H \left\{ 1 - \frac{\phi_1 \sinh k(x-l) + \phi_2 \sinh kx + \phi_3 \cosh kx}{\phi_2 \sinh kl + \phi_3 \cosh kl} \right\}, \quad (2)$$

$$u_1 = \frac{\sigma_n}{kE_1(1+\beta)} \times \left\{ \frac{\phi_1 (\cosh k(x-l) + 1) + \phi_2 \cosh kx + \phi_3 \sinh kx + \phi_4 \cosh kl + \phi_5 \sinh kl}{\phi_2 \sinh kl + \phi_3 \cosh kl} + k\beta x \right\}, \quad (3)$$

$$u_2 = \frac{\sigma_n}{kE_1(1+\beta)} \times \left\{ k\beta x - \frac{\phi_1 (\beta \cosh k(x-l) - 1) + \phi_2 \beta \cosh kx + \phi_3 \beta \sinh kx + \phi_4 \cosh kl + \phi_5 \sinh kl}{\phi_2 \sinh kl + \phi_3 \cosh kl} \right\}, \quad (4)$$

$$\tau_0 = \sigma_n \alpha k \left\{ \frac{\phi_1 \cosh k(x-l) + \phi_2 \cosh kx + \phi_3 \sinh kx}{\phi_2 \sinh kl + \phi_3 \cosh kl} \right\}, \quad (5)$$

where,

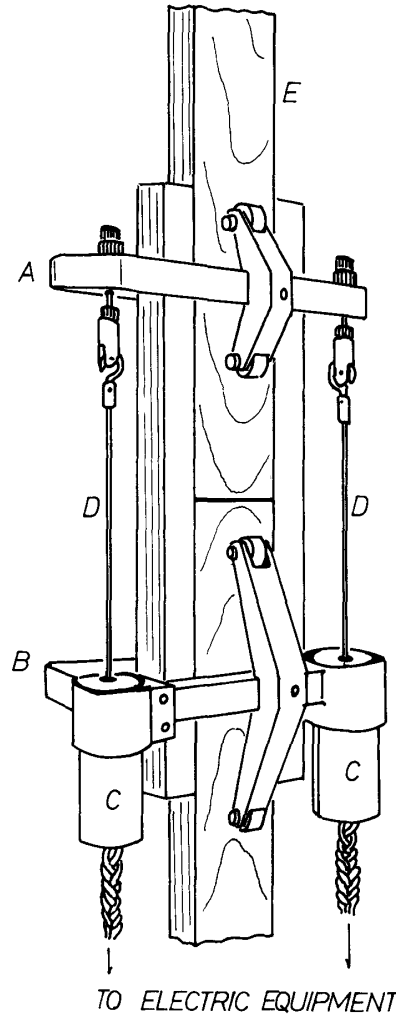


Fig. 2. Extensometer fitted on a double lap joints specimen. A: upper knife holder, B: lower knife holder, C: differential transformer, D: non-conducting rod, E: specimen.

$$\begin{aligned} \psi_1 &= kt_b\beta(1-R), & \psi_2 &= kt_b(1+\beta R), & \psi_3 &= R(1+\beta), \\ \psi_4 &= kt_b\beta(\beta+R), & \psi_5 &= k^2t_b^2\beta(1+\beta), & R &= E_b/E_1, \\ \beta &= (E_1B_1)/(E_2B_2), & 1/\alpha &= (1+\beta)/B_1, & k^2 &= (\lambda/E_1)(1/\alpha), \end{aligned} \quad (6)$$

and E is Young's modulus, B is width of adherend, subscripts 1, 2, 0, and b indicate adherend-1, 2, glue line, and butt joint respectively. H and $2t_b$ are thickness of specimen and thickness of butt joint respectively.

In eqs. (1)~(6), variables except λ are known. The only unknown factor λ was introduced to relate the apparent shear stress τ_0 in glue line of negligible thickness with relative displacement of adherends $u_1 - u_2$ (see APPENDIX). This factor λ was determined experimentally as follows:

First, the apparent displacement at appropriate locations of adherend-1 ($x=L$, see Fig. 1) was measured by an extensometer of differential transformer type as shown in Fig. 2. Then, by comparing measured displacement per unit stress $2u_1(L)/\sigma_n$ with calculated one in which $u_1(L)$ was obtained by substituting various values of E_1/λ into eq. (3), the value of E_1/λ which satisfy the experimental data was determined. Fig. 3 shows an example of this comparison of calculated displacement

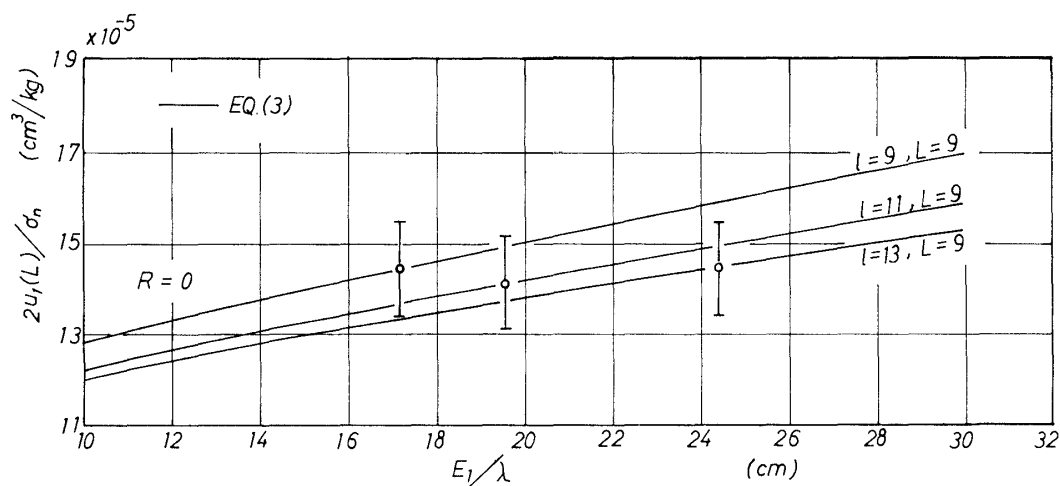


Fig. 3. Relation between displacement per stress $2u_1(L)/\sigma_n$ and ratio E_1/λ . l : half lap length, L : location of knifedge of extensometer. Each plot indicates mean and standard deviation of 2~5 specimens.

per unit stress (solid line in Fig. 3) with measured one. By averaging thirty experimental data, the value of E_1/λ was determined as 18 cm. Hence the value of λ was about $8.5 \times 10^3 \text{ kg/cm}^3$, because mean value of E_1 used these experiments was $150 \times 10^3 \text{ kg/cm}^2$.

On the other hand, it was assumed that fracture of the double lap joints started at the point FP_I or FP_{II} in Fig. 1, and that when the apparent strain energy release rate G^* of the double lap joints reached its critical value G_c^* , fracture of the joints

occured. In order to estimate the apparent strain energy release rate G^* , so-called J-integral method was applied. According to Rice^(7),8), the J-integral is expressed as follows:

$$J = G^* = \int_{\Gamma} \left(W dy - T \frac{\partial U}{\partial x} ds \right), \quad (7)$$

where, W is strain energy density function in two dimensional body and expressed as:

$$W = \int (\sigma_x d\epsilon_x + \sigma_y d\epsilon_y + \tau_{xy} d\gamma_{xy}),$$

here, σ_x , σ_y and τ_{xy} are stress components and ϵ_x , ϵ_y and γ_{xy} are strain components in the body respectively, T is traction vector on the path Γ and expressed as:

$$\begin{aligned} \mathbf{T} = [\mathbf{X}_v, \mathbf{Y}_v] &= [\sigma_x \mathbf{n} + \tau_{xy} \mathbf{m}, \tau_{xy} \mathbf{n} + \sigma_y \mathbf{m}], \\ \mathbf{n} &= dy/ds, \quad \mathbf{m} = -dx/ds. \end{aligned}$$

U is displacement vector on the path Γ and expressed as:

$$\mathbf{U} = [u, v]^T,$$

here, u and v are displacements in the body. Γ is arbitrary path surrounding the notch tip as shown in Fig. 4.

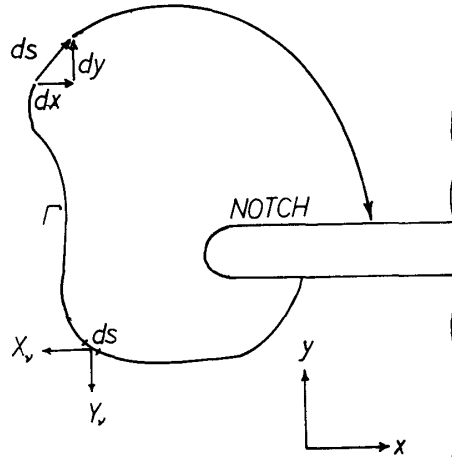


Fig. 4. Notched body and path Γ of J-integral.

In the double lap joints specimen considered here, the path Γ was drawn so as to be parallel to x-axis and/or y-axis surrounding the expected fracture point FP_1 in Fig. 5. By choosing the path in this way, J-integral can be split into two equations, one of which holds good to the partial path Γ_x parallel to x-axis, and the other holds good to the partial path Γ_y parallel to y-axis, namely:

$$J_x = - \int_{\Gamma_x} \left(\tau_{xy} \epsilon_x + \sigma_y \frac{\partial v}{\partial x} \right) dx, \quad (8)$$

$$J_y = \int_{\Gamma_y} \left\{ \frac{1}{2} (S_{11} \sigma_x^2 + 2S_{12} \sigma_x \sigma_y + S_{22} \sigma_y^2 + S_{33} \tau_{xy}^2) - (\sigma_x \epsilon_x + \tau_{xy} \frac{\partial v}{\partial x}) \right\} dy, \quad (9)$$

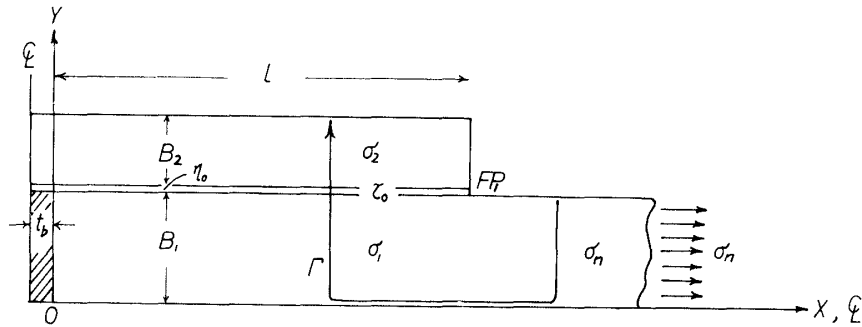


Fig. 5. Path Γ of J-integral at one right-angled corner FP_1 of the double lap joints specimen including a butt joint.

where, $S_{11} \sim S_{33}$ are elastic compliances of orthotropic body. In the approximate analysis conducted here, stress are not functions of y but of x only, hence J-integral takes following simple form:

$$J = J_y = \frac{1}{2} \{ (B_1/E_1)\sigma_1^2(x) + (B_2/E_2)\sigma_2^2(x) - (\eta_0/G_0)\tau_0^2(x) - (B_1/E_1)\sigma_n^2 \}, \quad (10)$$

where, G_0 and η_0 are imaginary shear rigidity and thickness of the glue line respectively and these were introduced to estimate apparent energy density in glue line. These can be related with the experimental factor λ as (see APPENDIX):

$$G_0/\eta_0 = \lambda. \quad (11)$$

Substituting stress components of eqs (1), (2), and (5), and eq. (11) into eq. (10), J-integral can be simplified in the form independent of x as follows:

$$J = G^* = \frac{\sigma_n^2 \alpha}{2E_1} \left\{ \frac{(\phi_2 \sinh kl + \phi_3 \cosh kl)^2 + 2\phi_1(\phi_2 \cosh kl + \phi_3 \sinh kl) + \phi_1^2 + \phi_2^2 - \phi_3^2}{(\phi_2 \sinh kl + \phi_3 \cosh kl)^2} \right\}, \quad (12)$$

Assuming that apparent strain energy release rate G^* of double lap joints is proportional to the strain energy release rate G measured on cracked adhesive joint specimens, following relation will be expected:

$$J = G^* = NG, \quad (13)$$

where, N is unknown coefficient. Hence the critical axial stress of adherend-1 can be obtained as follows:

$$\sigma_{nc} = \sqrt{2NG_c E_1 / \alpha} \times \frac{\phi_2 \sinh kl + \phi_3 \cosh kl}{\sqrt{(\phi_2 \sinh kl + \phi_3 \cosh kl)^2 + 2\phi_1(\phi_2 \cosh kl + \phi_3 \sinh kl) + \phi_1^2 + \phi_2^2 - \phi_3^2}}. \quad (14)$$

In the latter sections, applicability of eq. (14) will be discussed by comparing with experimental results.

Experimental

Specimen Preparation and Test Method

Adherend: Lawson cypress (*Chamaecyparis Lawsoniana* PARL.).

Adhesive: Epoxy adhesive which is mixture of bisphenol-A of WPE* 180~190 and dibutylphthalate.

Hardner: 11 phr** of diethylenetriamine (DETA).

Curing condition: Room temperature.

The mechanical properties of Lawson cypress and cured epoxy resin used in this study are tabulated in Table 1.

Table 1. Young's modulus of materials used in this study.

Lawson cypress	Epoxy adhesive
E_x (kg/cm ²)	E_b (kg/cm ²)
150×10^3	25×10^3

Mixed epoxy adhesive was warmed at about 50°C and removed bubbles and spread on a radial surface of each air-dried wood blocks by a spatula. Two center blocks were paired to make a thin slit between their end surfaces and two splint blocks were lapped over the center blocks as shown in Fig. 1 and these were clamped by several large clips. After about a day, clips were removed and double lap joints specimens were finished. Same epoxy adhesive used above was poured into the center slit of the finished specimen the bottom of which was sealed with cellulose tape to make a glued butt joint in response to the necessity. In the series of experiments, length of unlapped parts of adherend-1 were fixed to 10 cm. Thickness of glue line of butt joint $2t_b$ was also kept constant by a teflon spacer shim of 0.15 cm thick. Half lap length l , width of adherends $2B_1$ and B_2 , and thickness of specimen H were varied in response to the experimental program.

Fracture test was conducted on a lever type testing machine (Mori Testing Machine Prod. Co. Ltd., 5 tons capacity). To determine the experimental factor λ , measurements of displacement were done on thirty specimens of different widths of adherend randomly selected from the total specimens. The extensometer and the fitting on a specimen are shown in Fig. 2. All tests were done in a room conditioned at about 20°C, 65 % R.H.

Results and Discussion

Relation between half Lap Length and Strength of Specimens with an unglued Butt Joint at the Center.

Figs. 6~9 show the relation between critical axial stress σ_{nc} and half lap length l of double lap joints specimens with an unglued butt joint at the center. The

* WPE weight per epoxy equivalent.

** phr parts per hundred of resin by weight.

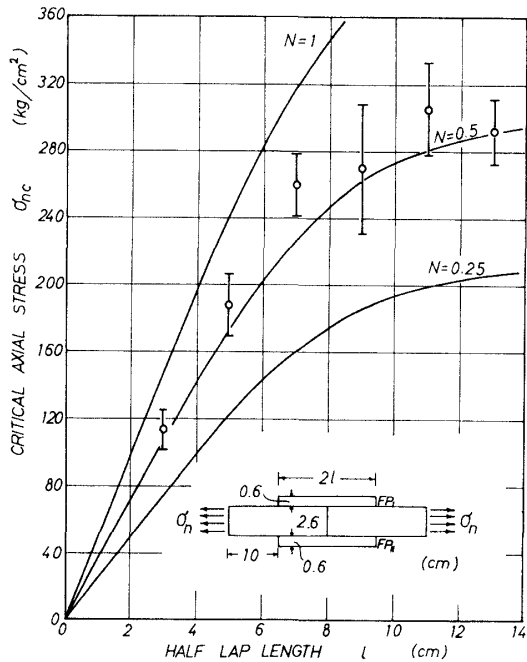


Fig. 6. Critical axial stress σ_{nc} of double lap joints specimens with an unglued butt joint and thin splints as a function of the half lap length l . Each plot indicates mean and standard deviation of 4~6 specimens. Solid curves indicate strength predicted with eq. (14).

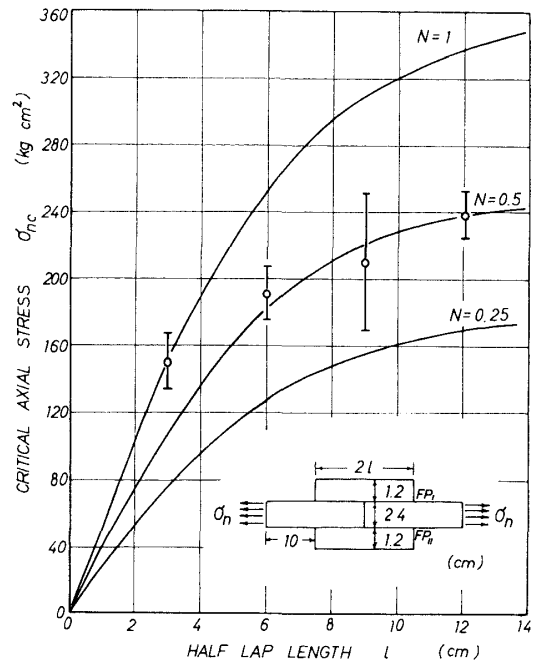


Fig. 7. Critical axial stress σ_{nc} of double lap joints specimens with an unglued butt joint and thick splints as a function of the half lap length l . Each plot indicates mean and standard deviation of 3 specimens. Solid curves indicate strength predicted with eq. (14).

solid curves in these figures indicate the strength predicted with eq. (14) by substituting 0.25, 0.5, and 1.0 as the value of unknown coefficient N and $0.25 \text{ kg}\cdot\text{cm}/\text{cm}^2$ as the basic value of fracture toughness of cracked adhesive joint system subjected to shear force²⁾. Similar results were obtained on half cut specimens with a thick gap of the center piece at the clamped end as is shown in the sub-figures (Figs. 8 and 9) to those of the specimens having lap length of $2l$ and with a thin slit at the center (Figs. 6 and 7). Considering the coincidence between experimental results and calculated ones, it may be concluded that the best applicability of eq. (14) can be performed when 0.5 is used as the coefficient N . Therefore, discussion will be done only on the case of $N=0.5$ after this.

Influence of Width of center Adherend

Influence of width of center adherend $2B_1$ on the strength of double lap joints is thought to be significant as well as the effect of lap length. Fig. 10 shows this influence on strength of double lap joints with calculated examples. It is suggested that the width of center adherend should be thin to give the higher strength. This suggestion may be applied to another composite wood like glued laminated wood or LVL.

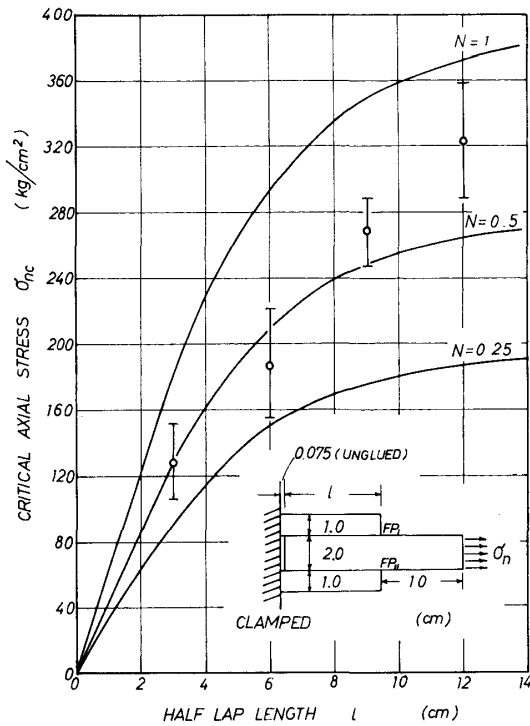


Fig. 8. Critical axial stress σ_{nc} of half cut lap specimens with thick side pieces and with a thick gap along one end of the center piece as a function of the half lap length l . Each plot indicates mean and standard deviation of 5 specimens. Solid curves indicate strength predicted with eq. (14).

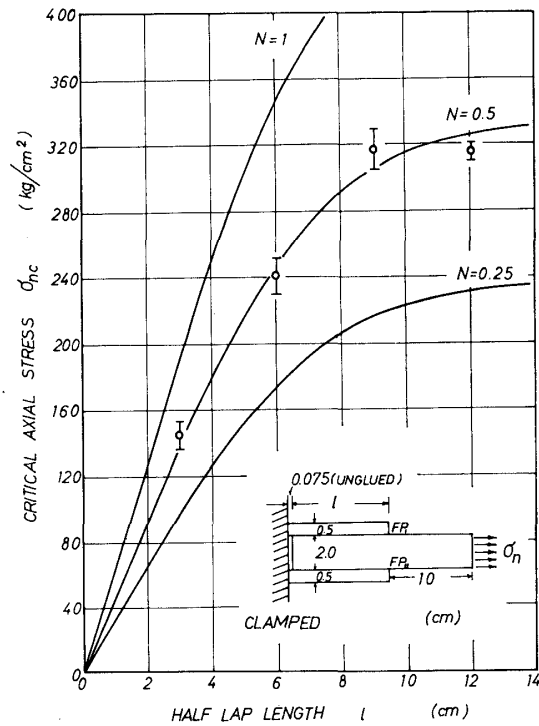


Fig. 9. Critical axial stress σ_{nc} of half cut lap specimens with thin side pieces and with a thick gap along one end of the center piece as a function of the half lap length l . Each plot indicates mean and standard deviation of 4 specimens. Solid curves indicate strength predicted with eq. (14).

Effect of Butt Joint on the Strength of Double Lap Joints.

Fig. 11 shows the relation between critical axial stress σ_{nc} and half lap length l for various stiffness ratio $R = E_b/E_1$, where E_b and E_1 are Young's modulus of glued butt joint and adherend-1 in x-direction, respectively. These calculations show that when the half lap length approaches to zero and R is larger than 0.02 fracture does not start at a corner FP_I or FP_{II} . In reality, however, partial separation at the glued butt joint always occurs prior to the breakdown of specimen. After once the butt joint separation takes place, ratio R becomes zero and the breakdown of specimen occurs when the axial stress reaches a value on the curve for $R=0$. Fig. 12 shows this progress of test on the different specimens. In this figure, the solid curves indicate the strength predicted with eq. (14) by substituting 0.5 for N and $0.25 \text{ kg}\cdot\text{cm}/\text{cm}^2$ for G_c . It can be seen that if partial separation at the glued butt joint occurs at stress level above the solid curve for $R=0$, whole specimen breakdown at this instance (see case of $l=3 \text{ cm}$), but even if partial separation at the glued butt joint occurs at stress below the solid curve for $R=0$,

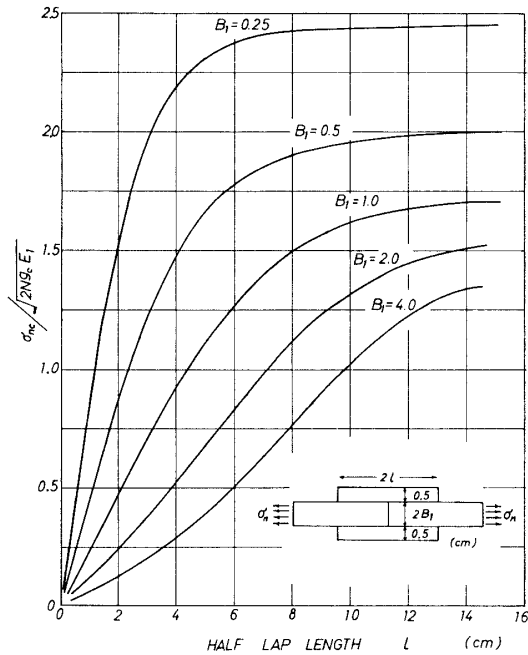


Fig. 10. Influence of width of center adherend on the strength of double lap joints with an un-glued butt joint. Solid curves indicate strength predicted with eq. (14).

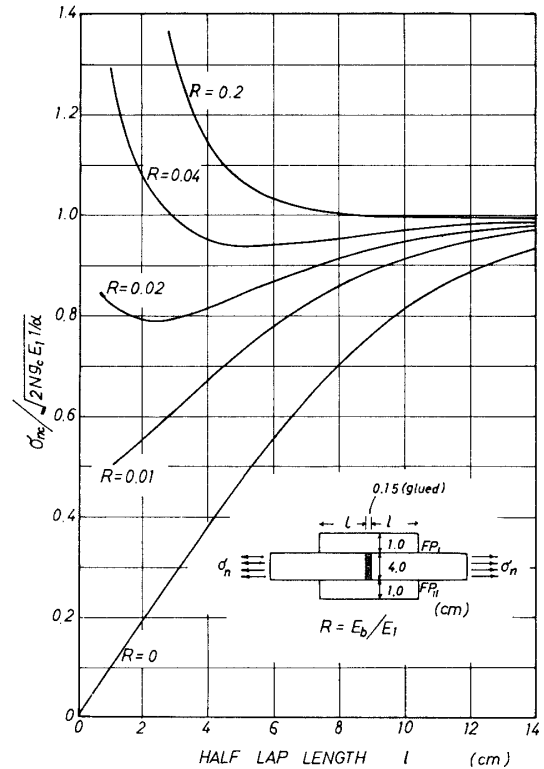


Fig. 11. Effect of stiffness of butt joint on the strength of double lap joints. Solid curves indicate strength predicted with eq. (14).

whole specimen does not break down till the axial stress reaches the solid curve for $R=0$ (see cases of $l=5\sim 11$ cm). As half lap length becomes longer, the probability of fracture at the point FP_I or FP_{II} before butt joint separation increases. This type of fracture is expected to bring the breakdown of whole specimen at once (see case of $l=13$ cm).

From these test results, it may be concluded that the existence of glued butt joint at the center of the specimen does not give sufficient efficiency to the maximum strength of double lap joints.

Design Equation of Glued Double Lap Joints

It is enough for designing double lap joints to consider only the case of $R=0$, even if the joints include an end glued butt joint. In this case, eq. (14) can be simplified by putting $\psi_3=0$ (i.e. $R=0$) as follows:

$$\sigma_{nc} = \sqrt{2NG_c E_1} / \alpha \left(\frac{\sinh kl}{\cosh kl + \beta} \right). \quad (15)$$

From the test results shown in Figs. 6~9, it appears that strength of the glued double lap joints is propotional to the joint aera when the half length is relatively short. This linear relation can be approximated by using an initial slope of eq. (15)

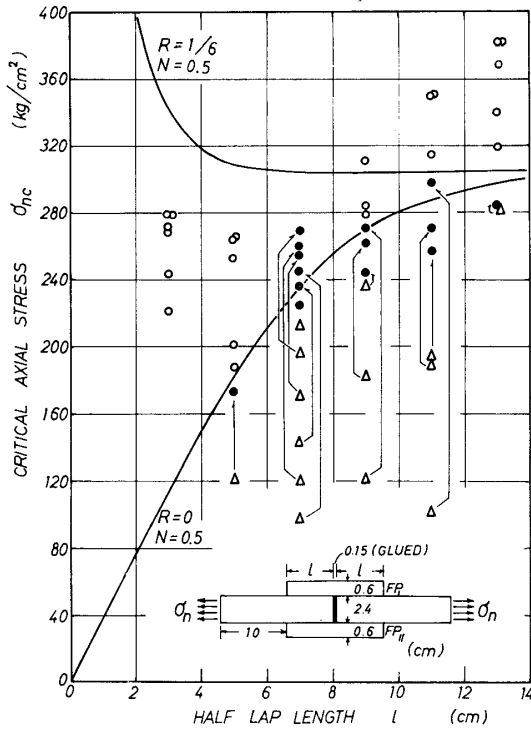


Fig. 12. Effect of stiffness of butt joint on the strength of double lap joints. Solid curves indicate strength predicted with eq. (14). \circ : breakdown of whole specimen, \bullet : breakdown of specimen after a glued butt joint separation, \triangle : partial separation at glued butt joint. Arrows indicate progresses from partial separation at glued butt joint to breakdown of whole specimen.

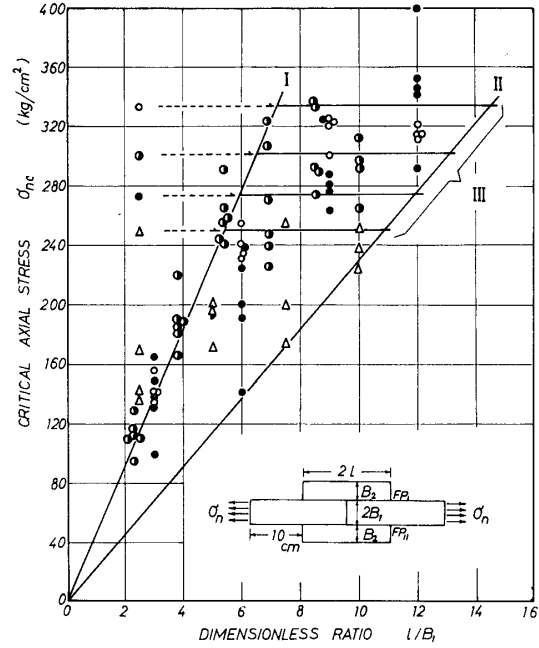


Fig. 13. Individual test result. Approximated linear relations between strength of double lap joints and aspect ratio l/B_1 (line-I and -II), and maximum strength of the joints (line-III). \circ : $B_1=1.0$, $B_2=0.5$ cm; \bullet : $B_1=1.3$, $B_2=0.6$ cm; \bullet : $B_1=B_2=1.0$ cm; \triangle : $B_1=B_2=1.2$ cm.

as:

$$\text{Initial slope} = \left. \frac{d\sigma_{nc}}{dl} \right|_{l=0} = \sqrt{2NG_c E_1 \alpha} \cdot k/B_1. \quad (16)$$

Thus, a linear relation between strength and aspect ratio l/B_1 can be derived from eq. (6) and eq. (16) as follows:

$$\sigma_{nc} \doteq \sqrt{2NG_c \lambda} \cdot (l/B_1). \quad (17)$$

On the other hand, strength of the joints reaches a maximum value gradually as the half lap length becomes longer. This limit value can be obtained easily by taking an infinite limit of eq. (15), namely:

$$\sigma_{\max} = \lim_{l \rightarrow \infty} \sigma_{nc} = \sqrt{2NG_c E_1 l / \alpha}. \quad (18)$$

In case of the joints made of same species of wood:

$$\sigma_{\max} = \sqrt{2NG_c E_x S}, \quad S = (B_1 + B_2)/B_1 B_2. \quad (19)$$

Fig. 13 shows the applicability of these approximate equations in case of

$N=0.5$ In this figure, line-I is eq. (17), line-II is the half value of line-I, and line-IIIs indicate the maximum strength of the joints calculated with eq. (19). It can be seen in this figure that the line-II gives good but somewhat conservative estimation of the joint strength to the aspect ratio l/B_1 , and that line-IIIs give rough estimation of the maximum strength of the joints to be expected. In consequence, it is reasonable to use the line-II as a design equation of the glued double lap joints, namely:

$$\sigma_{ne} = 0.5 \sqrt{G_c \lambda} \cdot (l/B_1). \quad (20)$$

Application limit of eq. (20) is given by eq. (19).

Conclusions

(1) Strength of the glued double lap joints could be deduced by applying Fracture Mechanics.

(2) It was hardly effective for the maximum strength of glued double lap joints to make an end glued butt joint with rigid adhesive.

(3) Width of adherends of double lap joints should be thin to get a high joint efficiency.

(4) Strength of double lap joints was proportional to the joint area when lap length was relatively short, but reached a maximum value gradually as lap length became longer. Considering these inclinations, the following design equation were proposed.

(a) Linear relation between strength and aspect ratio l/B_1 :

$$\sigma_{ne} = 0.5 \sqrt{G_c \lambda} \cdot (l/B_1), \quad \lambda = E_x/25 \sim E_x/15.$$

(b) Maximum strength to be expected:

$$\sigma_{max} = \sqrt{G_c E_x S}, \quad S = (B_1 + B_2)/B_1 B_2.$$

APPENDIX

Determination of Stress and Displacement of Double Lap Joints

[I] Assumption of apparent shear stress in glue line.

$$\tau_0 = \lambda(u_1 - u_2) \quad (A1)$$

[II] Equilibrium equations of forces acting in x-direction.

$$\frac{dN_1}{dx} - \tau_0 H = 0 \quad (A2)$$

$$\frac{dN_2}{dx} + \tau_0 H = 0 \quad (A3)$$

[III] Hooke's laws in adherends.

$$N_1/(B_1 H) = E_1 \frac{du_1}{dx} \quad (A4)$$

$$N_2/(B_2 H) = E_2 \frac{du_2}{dx} \quad (A5)$$

In the combination of relatively rigid adherends and fairly thick layers of elastomeric adhesive, the shear stress in adhesive layer is defined as $\tau_0 = G_0/\eta_0 (u_1 - u_2)$. But in case of wood adhesive joint system with negligibly thin and rigid glue line, it is difficult to define τ_0 as above expression if Volkersen type analysis dare to be used. Therefore the apparent shear stress was assumed to have the form as shown in eq. (A1), and λ was introduced to obtain the closed form solutions which enable to calculate the J-integral.

From eqs. (A1)~(A5), differential equation of τ_0 is obtained as follows:

$$\frac{d^2\tau_0}{dx^2} - k^2\tau_0 = 0, \quad (A6)$$

where, $k^2 = (\lambda/E_1)(1/\alpha)$, $1/\alpha = (1+\beta)/B_1$, $\beta = (E_1B_1)/(E_2B_2)$ (A7)

General solution of eq. (A6) is

$$\tau_0 = C_1 e^{kx} + C_2 e^{-kx}. \quad (A8)$$

Substituting eq. (A8) into eqs. (A2) and (A3), we get

$$N_1 = (H/k)(C_1 e^{kx} - C_2 e^{-kx}) + C_3, \quad (A9)$$

$$N_2 = -(H/k)(C_1 e^{kx} - C_2 e^{-kx}) + C_4. \quad (A10)$$

Furthermore, substituting eqs. (A9) and (A10) into eqs. (A4) and (A5), and using the relations of eq. (A7) we get

$$u_1 = \frac{1}{\lambda(1+\beta)}(C_1 e^{kx} + C_2 e^{-kx}) + \frac{C_3 x}{E_1 B_1 H} + C_5, \quad (A11)$$

$$u_2 = \frac{-\beta}{\lambda(1+\beta)}(C_1 e^{kx} + C_2 e^{-kx}) + \frac{C_4 x}{E_2 B_2 H} + C_6. \quad (A12)$$

where, $C_1 \sim C_6$ are constants of integration.

Substituting eqs. (A11), (A12) and (A8) into eq. (A1), the following relations are obtained.

$$C_3 = C_4 \beta, \quad (A13)$$

$$C_5 = C_6. \quad (A14)$$

[IV] Boundary conditions.

at $x=0$; $N_1/(B_1 H) = E_b(u_1/t_b),$ (A15)

$$N_2/(B_2 H) = E_2(u_2/t_b), \quad (A16)$$

at $x=l$: $N_1/(B_1 H) = \sigma_n,$ (A17)

$$N_2 = 0. \quad (A18)$$

Substituting eqs. (A9)~(A12) with relations of eqs. (A13), (A14) into eqs. (A15) and (A16), and eliminating C_5 , the constant C_4 can be expressed with C_1 and C_2 as follows:

$$C_4 = \left(\frac{\phi_2 + \phi_3}{\phi_1} \right) \frac{H C_2}{k} - \left(\frac{\phi_2 - \phi_3}{\phi_1} \right) \frac{H C_1}{k}, \quad (A19)$$

where, $\phi_1 = k t_b \beta (1 - R)$, $\phi_2 = k t_b (1 + \beta R)$, $\phi_3 = R (1 + \beta)$,

and $R = E_b/E_1.$ (A20)

Thus, N_1 and N_2 can be expressed as:

$$N_1 = \frac{H}{k} (C_1 e^{kx} - C_2 e^{-kx}) + \frac{\beta HC_2}{k} \left(\frac{\psi_2 + \psi_3}{\phi_1} \right) - \frac{\beta HC_1}{k} \left(\frac{\psi_2 - \psi_3}{\phi_1} \right), \quad (A21)$$

$$N_2 = \frac{-H}{k} (C_1 e^{kx} - C_2 e^{-kx}) + \frac{\beta HC_2}{k} \left(\frac{\psi_2 + \psi_3}{\phi_1} \right) - \frac{\beta HC_1}{k} \left(\frac{\psi_2 - \psi_3}{\phi_1} \right). \quad (A21)$$

Constants of integration C_1 and C_2 can be determined by substituting eqs. (A21) and (A22) into the boundary condition of eqs. (A17) and (A18). Then, C_4 is obtained from eq. (A19). Those are

$$C_1 = \sigma_n k \alpha \left\{ \frac{\phi_1 e^{-kl} + (\psi_2 + \psi_3)}{(\psi_2 + \psi_3) e^{kl} - (\psi_2 - \psi_3) e^{-kl}} \right\}, \quad (A23)$$

$$C_2 = \sigma_n k \alpha \left\{ \frac{\phi_1 e^{kl} + (\psi_2 - \psi_3)}{(\psi_2 + \psi_3) e^{kl} - (\psi_2 - \psi_3) e^{-kl}} \right\}, \quad (A24)$$

$$C_4 = \sigma_n \alpha H. \quad (A25)$$

Finally, C_5 can be obtained from eq. (A15) or eq. (A16) by using C_1 , C_2 , and C_4 as:

$$C_5 = \frac{\sigma_n}{E_1 k (1 + \beta)} \left(\frac{\phi_4 \cosh kl + \phi_5 \sinh kl + \phi_1}{\phi_2 \sinh kl + \phi_3 \cosh kl} \right), \quad (A26)$$

where,

$$\phi_4 = kt_b \beta (\beta + R), \quad \phi_5 = k^2 t_b^2 \beta (1 + \beta). \quad (A27)$$

Hence, every component of axial stress, shear stress, and displacement can be determined.

References

- 1) H. SASAKI, Setschaku (Adhesion & Adhesive), **18**, 172 (1974).
- 2) K. KOMATSU, H. SASAKI and T. MAKU, Wood Research, No. 57, 10 (1974).
- 3) K. L. W. HARISCHANDRA and Y. OKOHIRA, The Bulletin of the Faculty of Agriculture, Mie University, No. 49, 107 (1975).
- 4) N. SUZUKI and Y. OKOHIRA, The Bulletin of the Faculty of Agriculture, Mie University, No. 50, 93 (1975).
- 5) K. KOMATSU, H. SASAKI and T. MAKU, Wood Research, No. 59/60, 80 (1976).
- 6) D. D. ELEY, Adhesion p. 207, Oxford University Press, London, (1961).
- 7) J. R. RICE, Fracture II, ed. by H. Liebowitz, p. 191, Academic Press, New York and London, (1968).
- 8) J. R. RICE, J. Appl. Mech., **35**, 379 (1968).